



ORIGINAL ARTICLE

Transient detection capabilities of small satellite gamma-ray detectors

Zsolt Bagoly¹ | Lajos G. Balázs^{2,3} | Gábor Galgóczi⁴ | Masanori Ohno^{4,5,2,6} |
András Pál² | Jakub Řípa^{5,4,7} | L. Viktor Tóth³ | Norbert Werner^{5,6,8}

¹Department of Physics of Complex Systems, Eötvös University, Budapest, Hungary

²Konkoly Observatory, RCAES, Hungarian Academy of Sciences, Budapest, Hungary

³Department of Astronomy, Eötvös University, Budapest, Hungary

⁴Institute of Physics, Eötvös University, Budapest, Hungary

⁵Lendület Hot Universe Research Group, MTA-Eötvös University, Budapest, Hungary

⁶School of Science, Hiroshima University, Hiroshima, Japan

⁷Astronomical Institute, Charles University, Prague, Czech Republic

⁸Department of Theoretical Physics and Astrophysics, Faculty of Science, Masaryk University, Brno, Czech Republic

Correspondence

Zsolt Bagoly, Department of Physics of Complex Systems, Eötvös University, Budapest, Hungary.
Email: zsolt.bagoly@elte.hu

Present address

Zsolt Bagoly, Department of Physics of Complex Systems, Eötvös University, H-1117 Budapest, Pázmány P. s. 1./A, Hungary.

Funding information

European Social Fund; European Union, KEP-7/2018; Hungarian Academy of Sciences, Lendület LP2016-11

Abstract

The new, small satellite-based gamma-ray detectors, like Cubesats Applied for MEasuring and Localizing Transients, will provide a new way to detect gamma transients in the multimessenger era. The efficiency and the detection capabilities of such a system will be compared with current missions, for example, Fermi Gamma-ray Burst Monitor (GBM). We used the Fermi GBM's observed short gamma-ray burst light curves aggregated from observed discrete detector event for the simulation input. The corresponding direction-dependent detector response matrices were used to generate photon counts and light curves around a simulated event, enabling to determine the statistics. This method can be used in the future for trigger algorithm and detector system development, and also to estimate the efficiency of the data analysis pipeline regarding the observable gamma-ray bursts' parameters as well as other electromagnetic transients.

KEYWORD

gamma rays: observations – instrumentation: detectors – space vehicles: instruments

1 | INTRODUCTION

As recent multimessenger gamma-ray burst Gamma-ray Burst Monitor (GRB) observations showed, it is critical to locate the gamma-ray source position with a high accuracy. That requires simultaneous precision timing measurements by several gamma observatories.

Due to the rising cost of space missions, only a handful of gamma-ray space observatories are launched per decade. However, miniaturization opens new opportunities for breakthrough science using CubeSats (nanosatellites), which are affordable also for small countries like Hungary. A constellation of CubeSats could perform both all-sky monitoring and timing-based localization of GRBs. Researchers at Eötvös University and Konkoly Observatory develop a new mission called Cubesats Applied for MEasuring and Localizing Transients (CAMELOT); Ohno et al. (2018); Pál et al. (2018); Torigoe et al. (2019); Řípa et al. (2018); Werner et al. (2018)). CAMELOT will enable all sky monitoring and fast localization of GRBs, thus providing key observational data on these exciting phenomena. The network of CubeSats is expected to detect about 300 GRBs per year and we have to be ready to take advantage of this opportunity. We work out a detailed science case for a number of detector placement versions, sizes, designs, for various numbers of satellites and varying orbital configurations.

Here, we analyze the transformations between two satellites' observations space on two levels. At first, we investigate the transformation between the BATSE and BeppoSAX GRBs' derived physical parameter space. Regarding the raw observed data, we propose a way to estimate the capacities of the planned CAMELOT detectors based on current Fermi GBM's gamma transient observations. This method can be used for detector development, trigger and data processing analysis.

2 | TRANSFORMATION OF THE GRBS' PHYSICAL PARAMETERS BETWEEN INSTRUMENTS

The T_{90} duration distribution of the BATSE GRBs (Horváth 1998) has shown that the Third BATSE Catalog duration distribution could be well fitted by a sum of three log-normal distributions. Similar analysis in the multidimensional parameter space suggests the existence of a short-intermediate-long group structure Balastegui et al. (2001); Hakkila et al. (2000); Mukherjee et al. (1998); Rajaniemi & Mähönen (2002). All these results suggest that the BATSE sample consists of three groups. However, the different spacecrafts' detectors had/have different spectral and trigger behavior, hence it is important to compare the physical quantities of the GRBs observed by different satellites and compare the results. Horváth (2009)

analyzed $T_{90}^{BeppoSAX}$ and identified the three groups: here, we compare the complete BeppoSAX GRBM's database (Guidorzi 2002; Rossi et al. 2007) with the BATSE GRBs.

During the analysis, we used the T_{90}^{BATSE} duration and the $H32$ spectral hardness variables in the Current BATSE Catalog for 1598 GRBs, similar to Horváth et al. (2006). In the BeppoSAX database (Guidorzi 2002) four common parameters were available for 1020 bursts: the $T_{90}^{BeppoSAX}$ duration, the HR spectral hardness, the $F_{tot}^{BeppoSAX}$ total fluence, and the $PeakC$ peak count, all these data were determined from the BeppoSAX observations. We identified three GRBs as outliers: OTB980427-15:40:30, OTB971206-21:57:44, and OTB980910-16:57:44.

The MCLUST R program package was used for mixture modeling and model-based clustering (<http://cran.r-project.org>). The method classifies the data (observed GRBs) into the classes, and re-iterate the groups' parameters on the members' data. A multidimensional normal distribution model was used to fit the data and the number of clusters was selected via Bayesian Information Criterion (BIC) with priors.

On the T_{90} - *hardness* plane, the BIC parameter unambiguously selects three groups for both the BATSE and the BeppoSAX data (Figure 1.) The different group membership probabilities specify the classification uncertainties: obviously they are largest at the common borders. The group parameters are also shown by the corresponding ellipses.

There are 289 common bursts in the BeppoSAX/BATSE database. Using these bursts one can determine the empirical transformation rule from the BeppoSAX's observed physical parameter space into the BATSE's observed physical parameters. This allows us to use identical (or at least very similar) definitions of the physical quantities in both satellites' observations.

Using these 289 common bursts' data, the following BeppoSAX \rightarrow BATSE parameter space multivariate linear transformation was fitted:

$$\begin{pmatrix} \log T_{90}^{tr} \\ \log H32^{tr} \end{pmatrix} = \mathbf{A} \begin{pmatrix} \log T_{90}^{BeppoSAX} - 1.0897 \\ \log HR + 0.1320 \\ \log F_{tot}^{BeppoSAX} - 0.5753 \\ \log PeakC - 0.9230 \end{pmatrix} + \begin{pmatrix} 1.2669 \\ 0.5300 \end{pmatrix}$$

where the transformation matrix is the following:

$$\mathbf{A} = \begin{pmatrix} 0.7875 & 0.3043 & 0.2142 & -0.3011 \\ -0.1246 & 1.7746 & 0.0656 & 0.01745 \end{pmatrix}$$

The T_{90}^{tr} parameter mainly depends on the $T_{90}^{BeppoSAX}$, but—due to the different detector and observation effects—the contribution from the hardness, fluence, and peak count is also significant. At the same time, $H32^{tr}$ depends only on the BeppoSAX's HR hardness while $T_{90}^{BeppoSAX}$ modifies

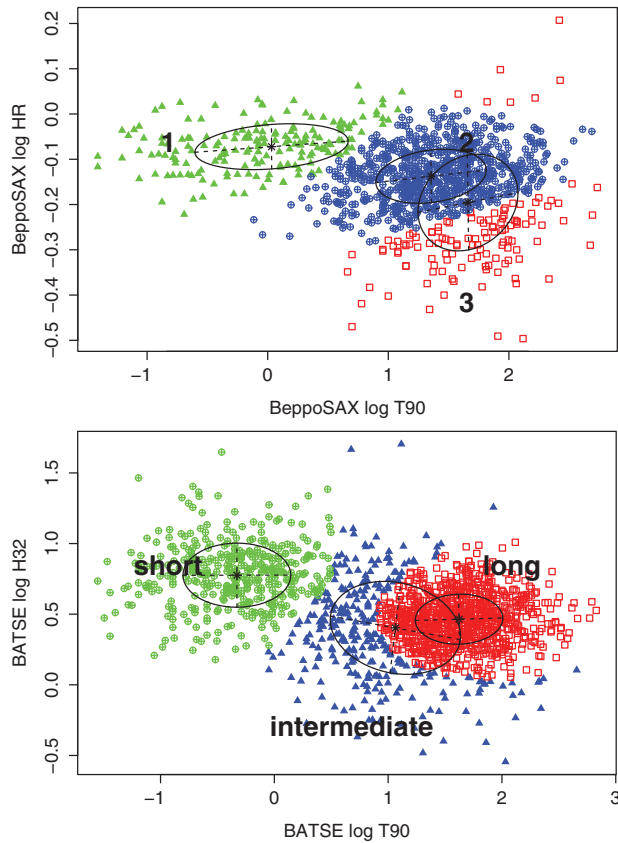


FIGURE 1 The three BeppoSAX and BATSE GRB groups found by MCLUST in the T_{90} - hardness plane

it only slightly. In Figure 2, the BATSE observed values are compared against the BATSE equivalent values, which were derived from the BeppoSAX's data using the multivariate linear approximation.

With this transformation, one can transform all BeppoSAX GRBs physical quantities into the BATSE equivalent (T_{90} , $H32$) space. Figure 3 shows the result of a new MCLUST classification. Due to the differences between the spacecrafts, the parameters of the fitted normal distributions were changed: the new group parameters are also shown by the corresponding ellipses.

The transformation allows us to plot the joint BATSE—GRBs together in Figure 4. It is quite remarkable that—according to the analysis—the BeppoSAX group 2 (the intermediate-like) is actually equivalent to the long BATSE group while BeppoSAX group 3 corresponds to the BATSE's intermediate one. N.B. it means that the red and blue color should be switched in Figure 1.

3 | TRANSIENT PREDICTION USING RAW EVENT TRANSFORMATION

To predict a detector efficiency, we usually use a series of simulations. At first, the Detector Response Matrix (DRM) is

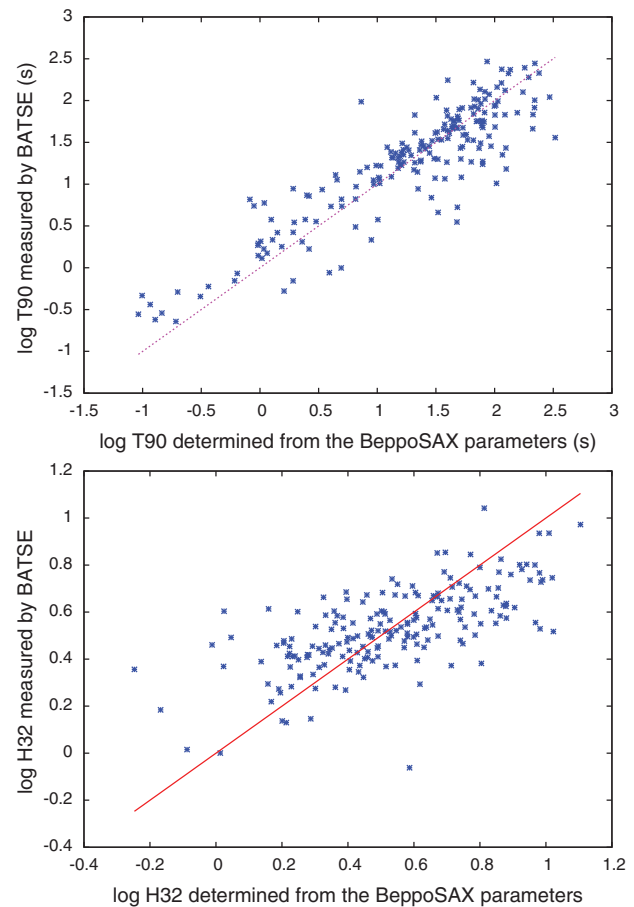


FIGURE 2 The BATSE equivalent T_{90}^{tr} and $H32^{tr}$ values determined from the BeppoSAX parameters and the real BATSE data

determined for a given physical and spacecraft configuration with the help of the particle physics (e.g., *GEANT*) software. The proper particle background estimation along the orbit provides the input for the observations' background: here, detailed analysis of the different components is needed (e.g., Szécsi et al. (2013); Szécsi et al. (2012); Řípa et al. (2018)). This will produce the background events that are time, orientation, and position dependent. The third component of the prediction is the supposed time-energy spectra of the source (e.g., GRB, solar flare, TGF, and SGR), which should be folded through the DRM to get the events we are looking for. For the simulation of the detection, several distributions should be assumed for, for example, geometrical parameters (detector-source direction, position of the Sun, Moon, and satellite orbit) or input source type and parameters (flux, fluence, hardness, and signal shape).

The parameters of the GRBs or other transients depend on the instrument, because transients should be triggered. The trigger parameters and methods are different from instrument to instrument, and usually hard to compare the efficiency of the different detectors. Here, we present a novel method for the estimation of a new detector efficiency using former observations and the new detector's DRMs.

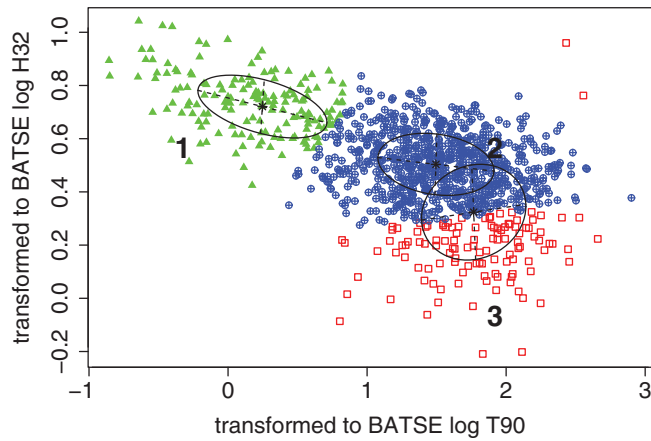


FIGURE 3 The classification of the transformed BeppoSAX dataset. Compare with Figure 1: the BeppoSAX group 2 is actually equivalent to the long BATSE group while BeppoSAX group 3 corresponds to the BATSE's intermediate one

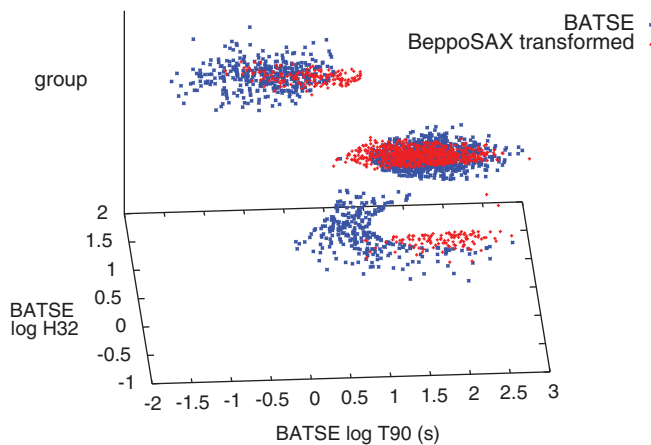


FIGURE 4 The short (1), intermediate (2), and long groups (3) of the transformed BeppoSAX catalog (red) and the original BATSE data (blue). Compare it with Figures 1. and 3.: the BeppoSAX group 2 transforms into the BATSE's long group, while BeppoSAX groups 3 corresponds to the BATSE's intermediate one

3.1 | The Fermi GBM detectors

The Fermi GBM detector system consists of 12 thallium activated Sodium Iodide (NaI(Tl)) and two Bismuth Germanate (BGO) scintillation detectors (Meegan et al. 2009). The NaI(Tl) detectors are sensitive to the low-energy spectrum (8 keV to ~ 1 MeV) while the BGO detectors cover the higher energy range of ~ 200 keV to ~ 40 MeV. The measured effective area of the detectors changes with the photon energy and the angle of incidence, with a maximum around ~ 100 cm² for NaI(Tl) and ~ 120 cm² for BGO detectors.

The photomultipliers' signals are analyzed on-board, classifying it with a pulse height analysis (PHA) into 128 PHA channels. The function between the incoming photon energy and the PHA channels is linear, described by the DRM. The geometry-dependent DRM contains the effective detection area as a function of all the parameters of geometry

(angular dependence of the efficiency, energy deposition and dispersion, atmospheric, and spacecraft scattering). The PHA distribution is usually wider for high-energy photons (especially above ~ 1 MeV), as some photons will scatter with the detector or spacecraft. The DRMs are provided as a standard data product for each GBM trigger, and there's a standard program package which allow to compute it for any given configuration. Here, we use the NaI(Tl) PHA energy channels, which have slightly different energy ranges from detector to detector, according to the detector's actual setup. These differences are usually minor, around or below 1 keV, hence here we use the same (mean) ranges for all the detectors. Our energy range covers 10 keV–960 keV. We leave out the 128th channel as it is the high-energy overflow channel. The low 10 keV limit reduces the background from soft events and weak variable X-ray sources.

Since November 2012, the GBM continuous time-tagged event (CTTE) data are available for each detector in 128 PHA energy channels (Meegan et al. 2009). For each detector and channel, the CTTE $2 \mu\text{s}$ event data are filtered with a 1 ms wide moving average filter, producing the light curve. This light curve could be used to produce accumulated background and event counts in a given time window.

An onboard trigger occurs when the count rates of two or more detectors exceed the background with a given threshold (4.5 – 7.5σ). The GBM trigger algorithms use different broad energy ranges (25–50 keV, 50–300 keV, 100–300 keV, and > 300 keV) and different timescales (from 16 ms to 8.192 s). A total of 120 different algorithms can be specified on the spacecraft, usually ~ 75 of them operate a given time.

3.2 | CAMELOT detectors

More than 15 alerts for candidates of the gravitational wave (GW) signal have been reported by the LIGO/Virgo collaborations since they have started publishing their GW detections via Gamma-ray Coordinate Network from April, 2019. Although many gamma-ray space-based instruments tried to detect electromagnetic signal counterparts to GW signals, no significant gamma-ray detection has been reported, except for the NS-NS merger event GW170817/GRB170817A. As these gamma-ray instruments basically consist of a single satellite, the position of GW signals is sometimes occulted by the earth and even instruments are switched off during their SAA passage (e.g., Fermi GBM detectors) or for the maintenance in some cases. This nondetection periods are non-negligible and can cause a sizeable fraction of the electromagnetic counterpart of GW sources to be missed.

All-sky coverage at any time of the GW detections and precise localization by gamma-ray observations is important for future GW or multimessenger astronomy. It is inevitable for single satellite to miss an instantaneous all-sky coverage at any time due to the earth occultation. Therefore, our

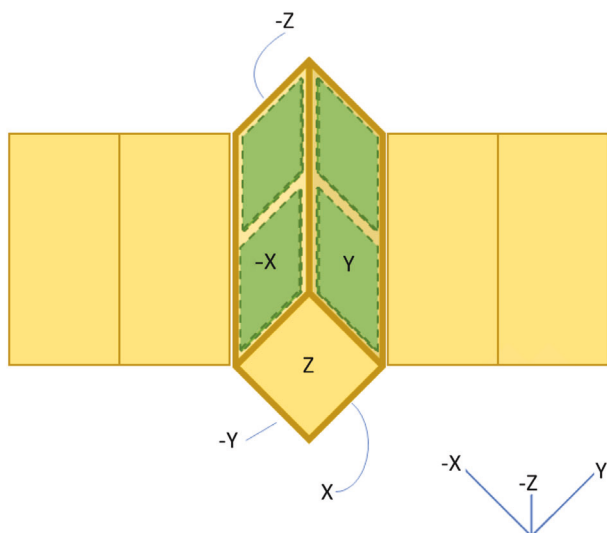


FIGURE 5 A possible CAMELOT detector configuration for four detectors in two-sided on 3 U CubeSat platform (modified Figure 3 of Werner et al. (2018))

proposing idea is to have a multiple set of detectors on the CubeSats and to localize the GW source position based on the arrival time difference of the gamma-ray photons with an accurate timing synchronization ($< 100 \mu\text{s}$). According to a simple triangulation principle of Hurley et al. (2013), the timing-based localization with such timing synchronization accuracy would result an $\sim 10'$ localization accuracy, which is useful for subsequent counterpart searches at other electromagnetic wavelengths (e.g., X-ray, optical, and radio). This mission concept has been developed and called the *CAMELOT* (Werner et al. (2018)). The basic idea of this mission is to have the gamma-ray detector on the 3 U CubeSat platform such as the platform developed for the RadCube mission by C3S LLC. The gamma-ray detector should have as large effective area as possible to increase the photon statistics for the timing-based localization. Considering the satellite platform, our baseline detector design is to put two to four thin, and relatively large ($8.3 \times 15 \text{ cm}^2$) CsI(Tl) scintillator on lateral extensions of the satellite platform as shown in Figure 5.

Each scintillator is readout by a multiple set of multipixel photon counter for its compactness, low-power consumption, and high signal to noise ratio. Figure 6 shows a current configuration of our single detector. Based on our ground experiments, this detector concept works very well with a good spectral performance. For instance, the lower-energy threshold of detecting photons of CAMELOT is found to be $\sim 10 \text{ keV}$ and the total effective area of four CAMELOT detectors is larger than 300 cm^2 for 100 keV photons (Torigoe et al. (2019)). Those performances are very similar to a single NaI detector of the Fermi-GBM. CAMELOT team also developed a simulation framework to evaluate the localization feasibility including detector performances, possible satellite platform and orbital configurations, and also actually observed timing

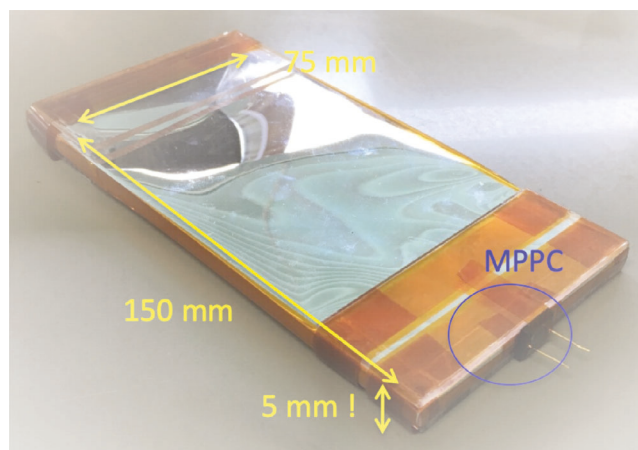


FIGURE 6 A picture of current design of the one detector of CAMELOT. A thin-large CsI(Tl) scintillator is enclosed by the reflecting material of Enhanced Specular Reflector and small photon counting device, MPPC is attached on the bottom part.(modified Figure 1 of Ohno et al. (2018))

and energy distributions of GRB photons by Fermi-GBM, etc (Ohno et al. 2018). This simulation study revealed that our mission concept based on the timing-based localization with a fleet of CubeSats could achieve 10-arcmin localization accuracy if we have at least nine sets of satellites. The CAMELOT detector is used not only for the localization of the electromagnetic counterpart of the GW sources, but also for detection of any other kinds of transients such as GRBs, solar flares, and terrestrial gamma-ray flashes because the detector performance is similar to that of single detector of the Fermi-GBM.

The CAMELOT DRM is calculated by a full Monte Carlo simulation based on GEANT4 (version 10.04) including 3 U CubeSats satellite geometry and four CsI scintillators enclosed by a 1 mm thickness Al casing. The input photon energy ranges from 10 to 1000 keV and we obtain an expected PHA channel distribution for CAMELOT. The CAMELOT DRM changes strongly depend on the incident angle of photons. Here, we just applied the incident angle where the CAMELOT DRM has the maximum effective area.

3.3 | Detector-to-detector transformation of the events

Generally, for the Fermi GBM and CAMELOT gamma scintillator detectors, one can simply describe numerically the particle to event count transformation as a matrix multiplication:

$$C = DRM \times E$$

where C is the vector of the detected counts in the detector PHA channels, E is the input energy spectrum with a given energy resolution, and DRM is the Detector Response Matrix for a given source and background geometry.

Here, our goal is to estimate the CAMELOT counts using real Fermi GBM's DRM and count data. The Fermi (NaI(Tl)) scintillation detectors cover different directions, therefore we have 12 such equations for the $i = 1 \dots 12$ C_i^{Fermi} count and the 12 DRM_i^{Fermi} DRM vectors. Our estimation will be the particle count in the CAMELOT detector PHA channels. Using the real observation means, we do not have to simulate neither GRB spectra with a given light curve nor the instrumental background spectra. However, this method will not take into account the different background and orbital variations, the spacecraft's material activation process, and will ignore the atmospheric scattering too.

For the Fermi GBM scintillators and the CAMELOT detector, we have

$$\begin{aligned} C_i^{Fermi} &= DRM_i^{Fermi} \times E \\ C^{CAMELOT} &= DRM^{CAMELOT} \times E \end{aligned}$$

here E is the (same) input spectrum.

We are looking for $C^{CAMELOT}$, which can be obtained formally:

$$C^{CAMELOT} = \sum_i DRM^{CAMELOT} \times (DRM_i^{Fermi})^{-1} \times C_i^{Fermi}$$

Usually, the GRB spectrum determination means a χ^2 -based forward folding fitting with a given energy model as calculating the proper $(DRM_i^{Fermi})^{-1}$ is hard, because usually it is ill-conditioned. Here, we have two similar matrices (the physics is not dissimilar) and one can observe that in reality we do not need the $(DRM_i^{Fermi})^{-1}$ matrix alone: instead of this, we need the $DRM^{CAMELOT} \times (DRM_i^{Fermi})^{-1}$ product that gives the solution. There is a method called Generalized Singular Value Decomposition that is able to accomplish this joint inverse and multiplication in one step.

The Generalized Singular Value Decomposition gives the following factorization for two general (A, B) matrices acting on a common input space:

$$\begin{aligned} A &= U \times \sum_A \times [0R] \times Q^T \\ B &= V \times \sum_B \times [0R] \times Q^T \end{aligned}$$

where U, V, Q are unitary matrices, Σ_A and Σ_B are diagonal matrices, and R is an upper triangular matrix. $[0R]$ means that it should be padded to get the right matrix sizes. One can observe that the procedure is very similar to the well-known Singular Value Decomposition, but here the two matrices will produce a joint R, Q transformation at first, acting on the common input space. There are several realizations of the algorithm, here we used the Octave Forge's *gsvd* routine in the *linear-algebra* package.

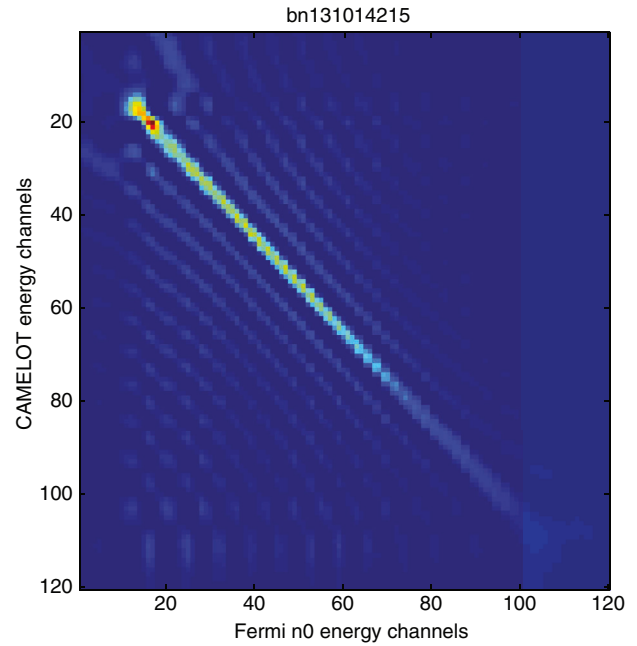


FIGURE 7 The Fermi \rightarrow CAMELOT count transform matrix for Fermi event bn131014215, detector 0

Let us have $A = DRM_i^{Fermi}$ and $B = DRM^{CAMELOT}$, then we will have

$$\begin{aligned} DRM^{CAMELOT} \times (DRM_i^{Fermi})^{-1} &= \\ &= V \times \sum^{CAMELOT} \times [0R] \times Q^T \times Q \times [0R]^{-1} \times \left(\sum_i^{Fermi} \right)^{-1} \\ &\times U^T = V \times \sum^{CAMELOT} \times \left(\sum_i^{Fermi} \right)^{-1} \times U^T \end{aligned}$$

R and Q cancel and in the middle the two diagonal matrices of the j^{th} element will be $\sum_j^{CAMELOT} / \sum_{i,j}^{Fermi}$, which is the j^{th} generalized singular value. This method can be used to create the necessary transform of the Fermi counts into the CAMELOT system.

The CAMELOT DRM depends on geometrical factors: here we will use the CAMELOT DRM for the best configuration with optimal detection direction/maximum effective area + 1 mm Al shielding, giving a good approximation of its best capacities. E.g. for Fermi trigger bn131014215, detector 0, the derived transition matrix can be seen in Figure 7.

One can observe that it is almost diagonal. There is a slight low-energy asymmetry, and it can be seen that the diagonal values drop at the higher-energy channels. The difference in the detector thickness will be important, as CAMELOT's thinner scintillators will be more transparent to the high energy photons. For the same event we can calculate the light-curve and channel distribution. Figure 8 shows the events in the 120 PHA channels during the original Fermi GBM observation, and Figure 9 shows what CAMELOT's detector would have seen for this GRB. The minor depletion of the high-energy

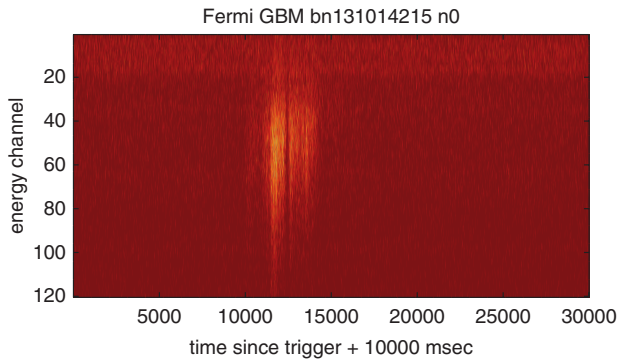


FIGURE 8 The Fermi GBM bn131014215, detector 0 event photon distribution in the original pulse height analysis (PHA) and time plane

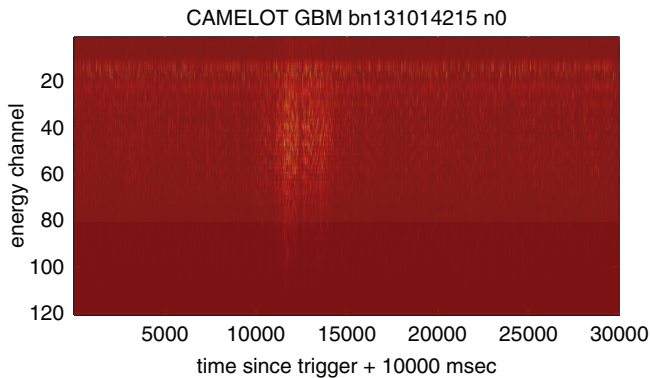


FIGURE 9 The Fermi GBM bn131014215, detector 0 event in the CAMELOT detector's pulse height analysis (PHA) - time plane

photons and the enhancement in the low energy channels is apparent in Figure 9.

Accumulating the counts among the energy channels between 10 keV-960 keV and detectors produces an overall light curve. In Figure 10, a weak GRB, Fermi GRB event bn100811108 light curve is shown, calculated from the original (blue) Fermi GBM counts and from the transformed (red) CAMELOT detector counts. This GRB had higher energy parts in the spectrum, therefore the CAMELOT light-curve is slightly lower during the event. The background is softer, hence did not show an observable difference.

Using similar algorithms, we can compare the overall detector efficiencies: for this, we used 776 GRB's from the Fermi GBM database with CTIME and DRM information, all of them with $T_{90} < 8$ s (GRB 170817A/GW170817 was classified as an intermediate GRB [Horváth et al. 2018]). Summing the counts for the energy channels between 10 keV and 960 keV, we obtained the light curves. As a simple criterion, we calculated the count in a 256 ms window in the background (this will give the N noise) and centered around the maximum (giving the S signal). Assuming the background to be approximately constant (for short burst it is a good approximation), the sum of the counts will follow a Poisson distribution. The average is high, so we can approximate it by

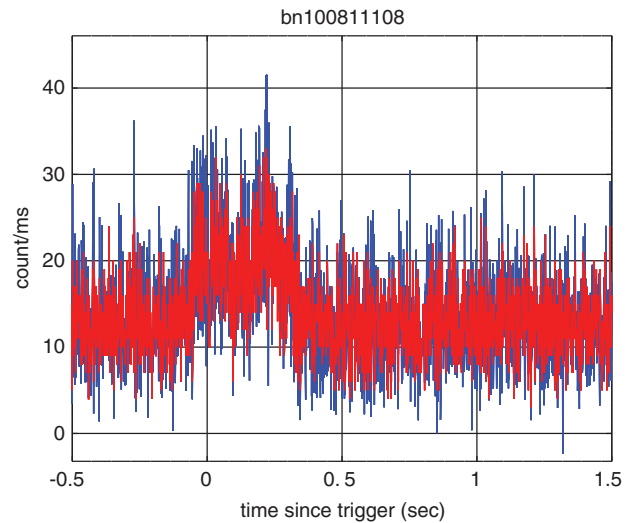


FIGURE 10 Light curve of bn100811108 calculated from the original (blue) Fermi GBM counts and from the transformed (red) CAMELOT counts

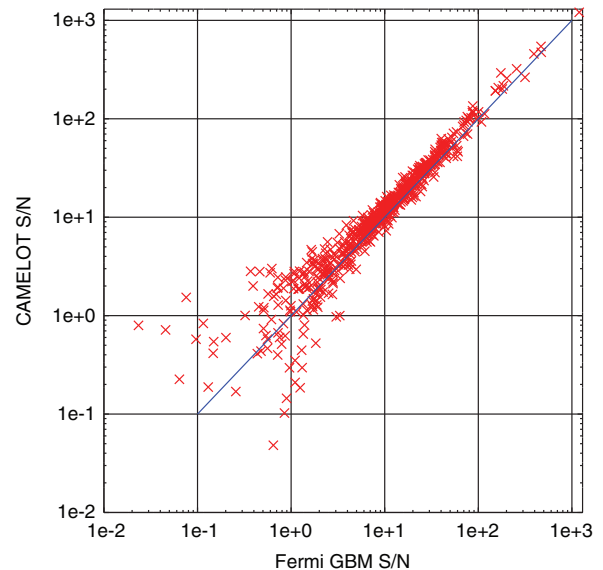


FIGURE 11 Signal-to-Noise ratio and detection efficiency for short-intermediate GRB in the Fermi GBM and CAMELOT scenario. Here, the best CAMELOT geometry was taken for the estimation

a Gaussian, hence the signal-to-noise ratio will be:

$$S/N = (S - N)/\sqrt{N}$$

In Figure 11, the Fermi GBM's and CAMELOT's efficiency for this simple trigger is shown. The CAMELOT's S/N values are systematically above the Fermi GBM's by 30%. The effective area of the optimal/best direction CAMELOT DRM is ≈ 2 times larger than Fermi GBM's, resulting a factor of $\approx \sqrt{2}$ in the S/N .

These points are all observed GRBs: the low S/N Fermi GBM values show the importance of the different trigger algorithm, covering wide ranges both in time and energy.

4 | CONCLUSIONS

Here, we presented two transformation methods acting on two satellites' observations space:

- We have shown on the joint BATSE/BeppoSAX GRB observations data that it is possible to transform the observed physical quantities (T_{90} , hardness) between the two spacecrafts. It helps the correct identifications of the GRB classes.
- We used the Generalized Singular Value Decomposition to transform the raw observed Fermi GBM event data into the CAMELOT detectors' space. It can be used to estimate the efficiency providing a tool for detector development, trigger and data processing analysis. N.B. this method did not incorporate all our knowledge about the sources and detectors (e.g., non-negativeness), therefore extending it with such constraints will probably improve them in the future.

ACKNOWLEDGMENTS

This research has been supported by the Hungarian Academy of Sciences and by the European Union via grants Lendület LP2016-11 and KEP-7/2018, and cofinanced by the European Social Fund: Research and development activities at the Eötvös Loránd University's Campus in Szombathely, EFOP-3.6.1-16-2016-00023.

CONFLICT OF INTEREST

The authors declare no potential conflict of interest.

AUTHOR CONTRIBUTIONS

All authors contributed extensively to the work presented in this article.

REFERENCES

- Balastegui, A., Ruiz-Lapuente, P., & Canal, R. 2001, *MNRAS*, 328, 283. <https://doi.org/10.1046/j.1365-8711.2001.04888.x>.
- Guidorzi, C. 2002. Ph.D. Thesis (Unpublished Doctoral Dissertation). University of Ferrara.
- Hakkila, J., Haglin, D. J., Pendleton, G. N., Malozzi, R. S., Meegan, C. A., & Roiger, R. J. 2000, *ApJ*, 538, 165. <https://doi.org/10.1086/309107>.
- Horváth, I. 1998, *ApJ*, 508, 757. <https://doi.org/10.1086/306416>.
- Horváth, I. 2009, *Ap&SS*, 323(1), 83. <https://doi.org/10.1007/s10509-009-0039-1>.
- Horváth, I., Balázs, L. G., Bagoly, Z., Ryde, F., & Mészáros, A. 2006, *A&A*, 447, 23. <https://doi.org/10.1051/0004-6361/20041129>.
- Horváth, I., Tóth, B. G., Hakkila, J., et al. 2018, *Ap&SS*, 363(3), 53. <https://doi.org/10.1007/s10509-018-3274-5>.
- Hurley, K., Pal'shin, V. D., Aptekar, R. L., et al. 2013, *ApJS*, 207, 39. <https://doi.org/10.1088/0067-0049/207/2/39>.
- Meegan, C., Lichti, G., Bhat, P. N., et al. 2009, *ApJ*, 702, 791. <https://doi.org/10.1088/0004-637X/702/1/791>.

- Mukherjee, S., Feigelson, E. D., Babu, G. J., Murtagh, F., Fraley, C., & Raftery, A. 1998, *ApJ*, 508, 314. <https://doi.org/10.1086/306386>.
- Ohno, M., Werner, N., Pál, A. et al. 2018, in: CAMELOT: Design and Performance Verification of the Detector Concept and Localization Capability. J.-W. A. den Herder, S. Nikzad, K. Nakazawa, Proc. SPIE, Vol. 10699, 1069964.
- Pál, A., Mészáros, L., Tarcai, N., et al. 2018, *arXiv*, 1806, 03685.
- Rajaniemi, H. J., & Mähönen, P. 2002, February, *ApJ*, 566, 202. <https://doi.org/10.1086/337959>.
- Řípa, J., Werner, N., Ohno, M. et al. 2018, Monitoring of gamma-ray bursts with a fleet of nanosatellites. 69th International Astronautical Congress, Bremen, Germany, pp. IAC-18,B4,2,8,x46335.
- Rossi, F., Carturan, D., Montanari, E., Frontera, F., & Guidorzi, C. 2007, *Il Nuovo Cimento B*, 121(12), 1571. <https://doi.org/10.1393/ncb/i2007-10310-2>.
- Szécsi, D., Bagoly, Z., Mészáros, A., Balázs, L. G., Veres, P., & Horváth, I. 2012, *MSAIS*, 21, 214.
- Szécsi, D., Bagoly, Z., Kóbori, J., Horváth, I., & Balázs, L. G. 2013, *A&A*, 557, A8. <https://doi.org/10.1051/0004-6361/201321068>.
- Torigoe, K., Fukazawa, Y., Galgóczi, G., et al. 2019, *Detect. Associat. Equip.*, 924, 316. <https://doi.org/10.1016/j.nima.2018.08.039>.
- Werner, N., Řípa, J., Pál, A. et al. 2018, CAMELOT: Cubesats Applied for MEasuring and LOCALising Transients mission overview. J.-W. A. den Herder, S. Nikzad, & K. Nakazawa. Proc SPIE, Vol. 10699, 106992P.

AUTHOR BIOGRAPHIES



Zsolt Bagoly was born in Szombathely, Hungary. He received his M.Sc. and Ph.D. degrees in physics from the Eötvös University, Budapest in 1986 and 1992, respectively. He is currently an Assistant Professor with the Department of Physics of Complex Systems, Eötvös University, Budapest. His current research interests include astrophysical data analysis, gamma-ray bursts, and cosmology.



Lajos György Balázs (1941) is an emeritus professor at the Konkoly Observatory and a privat professor at the Eötvös Loránd University. His main interest is the application of multivariate statistics on several astrophysical problems, including

star formation and gamma ray bursts (GRB). His team discovered a giant infrared ring in the Cepheus constellation, the Cepheus Bubble, based on the data of the IRAS satellite. The angular diameter of the Bubble is 10 degrees on the sky, corresponding to 150 pc and it connects several places of intense star formation. With his collaborators he discovered the largest regular formation in the observable Universe; a ring with a diameter of 1720 Mpc, displayed by 9 gamma-ray bursts (GRBs), exceeding by a factor of 5 the transition scale to the homogeneous and isotropic distribution of the cosmic matter.



Gábor Galgóczi was born in Budapest, Hungary in 1993. He received the BSc and MSc degrees in physics and astrophysics from the Eötvös Loránd University, Budapest, Hungary in 2015 and 2018 respectively. He currently

holds a Young researcher position at the Wigner Research Centre for Physics besides obtaining a PhD degree at the Eötvös Loránd University. He has been working in particle detector R&D since 2013. He is responsible for the development of particle simulations for the CAMELOT CubeSat mission, mainly investigating the activation and the background induced by trapped and cosmic particles in Low Earth Orbit. Besides working on simulations he has developed the track reconstruction algorithm for a Time Projection Chamber and has been involved in the optimization of a novel neutron detector and several muon detectors.



Masanori Ohno Senior Researcher at the Institute of Physics, Eötvös University His research fields of expertise are the X-ray and gamma-ray data analysis, developing a Monte Carlo method and instruments for extragalactic compact objects such as gamma-ray bursts (GRBs) and active galactic nuclei (AGN). Currently he's focusing on the CubeSat project called CAMELOT.



András Pál was born in Budapest, Hungary in 1981. He graduated from ELTE, MSc in physics (particle physics) and MSc in astronomy in 2004. His current status: research fellow at the Konkoly Observatory of the Hungarian

Academy of Sciences, PI of Fly's Eye (<http://flyseye.net>), a hexapod-based multi-color time-domain full-sky survey. His scientific interests and experiences cover low-level astronomical data reduction algorithms and implementations (optical and near-infrared photometry, astrometry and cross-matching, far-infrared photometry); small bodies in the Solar System: optical photometry, precise and accurate time series photometry and thermal radiation measurements, surface modelling, statistical analysis; extrasolar planets: discovery, characterization, follow-up measurements, parameter estimations and regression analysis, modelling of observables, dynamical analysis; electronics design and embedded programming (at the level of MCUs, ASICs, SoCs).



Jakub Řípa received the Master's degree in physics in 2006 and the Ph.D. degree in astronomy and astrophysics in 2011, both at the Charles University (MFF UK), Prague, Czech Republic under the supervision of doc. RNDr. Attila

Mészáros, DrSc. He was a postdoctoral researcher at: Institute for the Early Universe, Ewha Womans University, Seoul, Korea (2011–2012); Institute of Basic Science, Sungkyunkwan University, Suwon, Korea (2012–2015); Leung Center for Cosmology and Particle Astrophysics, National Taiwan University, Taipei, Taiwan (2015–2017). Currently, he is a postdoctoral researcher at the Astronomical Institute, Charles University and at the Lendület Hot Universe Research Group, MTA-Eötvös University, Budapest, Hungary. His research interests include gamma-ray bursts and instrumentation for high-energy astrophysics in hard X-rays and gamma-rays.



Viktor L. Tóth Ass. Prof. at the Dept. of Astronomy, Eötvös University. His scientific interests are Planck Galactic Cold Cores, Star formation and young stellar objects (YSOs) and Extragalactic and high energy astrophysics.



Norbert Werner is an astrophysicist, the leader of the *Lendület Hot Universe* research group at Eötvös Loránd University in Budapest, Hungary, an associate professor (Docent) in the Department of Theoretical Physics and Astro-

physics at Masaryk University in Brno, Czech Republic, and a specially appointed associate professor in the School of Science at Hiroshima University, Japan. Using mainly space observatories, but also ground based and airborne telescopes, he studies the hottest places and the most energetic phenomena in the Universe, such as the interaction of the hot atmospheres of galaxies, groups and clusters of galaxies with accreting supermassive black holes and the origin of elements. He is co-leading the development of the CAMELOT nano-satellite mission to monitor the gamma-ray sky.

How to cite this article: Bagoly Z, Balázs LG, Galgóczi G, et al. Transient detection capabilities of small satellite gamma-ray detectors. *Astron. Nachr.* 2019;340:681–689.

<https://doi.org/10.1002/asna.201913675>